

UC Irvine

UC Irvine Previously Published Works

Title

The nonlinear saturation of beam-driven instabilities: Irregular bursting in the DIII-D tokamak

Permalink

<https://escholarship.org/uc/item/5bh9d3m8>

Journal

Physics of Plasmas, 1(12)

ISSN

1070-664X

Authors

Heidbrink, WW
Danielson, JR

Publication Date

1994-12-01

DOI

10.1063/1.870822

Copyright Information

This work is made available under the terms of a Creative Commons Attribution License, available at <https://creativecommons.org/licenses/by/4.0/>

Peer reviewed

BRIEF COMMUNICATIONS

The purpose of this Brief Communications section is to present important research results of more limited scope than regular articles appearing in *Physics of Plasmas*. Submission of material of a peripheral or cursory nature is strongly discouraged. Brief Communications cannot exceed three printed pages in length, including space allowed for title, figures, tables, references, and an abstract limited to about 100 words.

The nonlinear saturation of beam-driven instabilities: Irregular bursting in the DIII-D tokamak

W. W. Heidbrink and J. R. Danielson

Department of Physics, University of California, Irvine, California 92717

(Received 13 July 1994; accepted 19 August 1994)

Intense fast-ion populations created by neutral-beam injection into a tokamak can destabilize fishbone modes and other instabilities. Regular, periodic bursts of fishbones often occur but, when another magnetohydrodynamic (MHD) mode is also unstable, the burst cycle is irregular. The complexity of the burst cycle over a long time scale correlates with the purity of the Fourier spectrum during a single burst (a short time scale). The data are consistent with a simple predator-prey model in which the second MHD mode introduces periodic perturbations into the evolution equations. © 1994 American Institute of Physics.

In tokamaks, superthermal ions injected by neutral beams can drive normal modes of the background plasma unstable. Several beam-driven instabilities are observed,¹ including fishbones, sawbones, toroidicity-induced Alfvén eigenmodes (TAE modes), and beta-induced Alfvén eigenmodes (BAE modes). These modes are of practical concern because they cause large, concentrated losses of the fast ions.¹ Potentially, instabilities driven by alpha particles could prevent ignition or damage the walls in a deuterium-tritium (D-T) reactor.

These beam-driven instabilities generally occur in bursts.¹ Heuristic predator-prey models (where the instability “preys” upon the beam-ion population by expelling fast ions) can reproduce experimentally observed fishbone cycles^{2–6} and can also account for most of the features of the TAE and BAE burst cycles.⁶ These semiempirical models predict a regular, periodic cycle. Although regular cycles are often observed experimentally, many burst cycles are irregular. This paper shows that an extended predator-prey model⁵ is consistent with experimental observations of irregular bursting.

In the DIII-D tokamak,⁷ bursts of fishbone activity are sometimes observed during beam injection.⁸ Unless TAE or BAE modes are also excited, fishbones are relatively weak in DIII-D, and small changes ($\leq 3\%$) in the volume-integrated 2.5 MeV neutron emission are produced. For this study, all discharges (through the 1993 campaign) with fast magnetics data (minimum 200 kHz sampling) that contain bursts of fishbone activity were examined. Three constraints on the data were imposed: (1) Toroidal field $B_T \geq 1.4$ T (to avoid strong TAE or BAE activity); (2) plasma current $I_p < 2.0$ MA (to avoid low q operation); (3) steady-state⁹ plasma conditions (to avoid variations in the burst cycle caused by evolution of the background plasma). With these constraints, 35 plasmas were selected that span the plasma conditions

$B_T = 1.4\text{--}2.1$ T, $I_p = 0.7\text{--}1.6$ MA, line-average density $\bar{n}_e = 2\text{--}8 \times 10^{13}$ cm⁻³, and beam power $P_B = 2.5\text{--}20$ MW.

Figure 1 shows the signal from a Mirnov loop for one of the discharges in our dataset. Regular bursts of fishbone activity are observed. Also shown in the figure is the fast Fourier transform (FFT) during one of the bursts. The dominant peak, which occurs at ~ 21 kHz, is an $n = 1$ kink mode. The $n = 2$ peak at ~ 41 kHz is a harmonic of the dominant peak caused by the nonsinusoidal shape of the fishbone oscillation. Closer examination of the time evolution of the bursts shows that the mode frequency gradually decreases through a burst, and this behavior accounts for the relatively broad peaks seen in the frequency spectrum. In addition to the dominant fishbone mode, there is another small $n = 1$ mode at ~ 17 kHz in this plasma. Examination of many spectra shows that the amplitude of this mode correlates weakly with the amplitude of the dominant fishbone mode.

Figure 2 shows an example of an irregular burst cycle. In this plasma, there are two $n = 1$ modes of roughly comparable amplitude, one near 26 kHz and the other near 31 kHz. Higher frequency harmonics of these modes are also evident in the spectrum.

These two examples are representative of a general trend: regular burst cycles occur for modes with a “pure” frequency spectrum, while erratic cycles correlate with complicated frequency spectra. In order to quantify this qualitative observation, we measure the amplitude of each burst A and the period between bursts T . For a 60 ms time record, 5–10 bursts are typical. We then calculate the mean \bar{A} and standard deviation δA of the amplitude data for this cycle, and perform a similar computation for the period data. The product $(\delta A \delta T)/(\bar{A} \bar{T})$ is a quantitative measure of the complexity of the cycle that is consistent with a qualitative assessment of irregularity. The uncertainty in $(\delta A \delta T)/(\bar{A} \bar{T})$ (associated with the selection of the 60 ms time window and

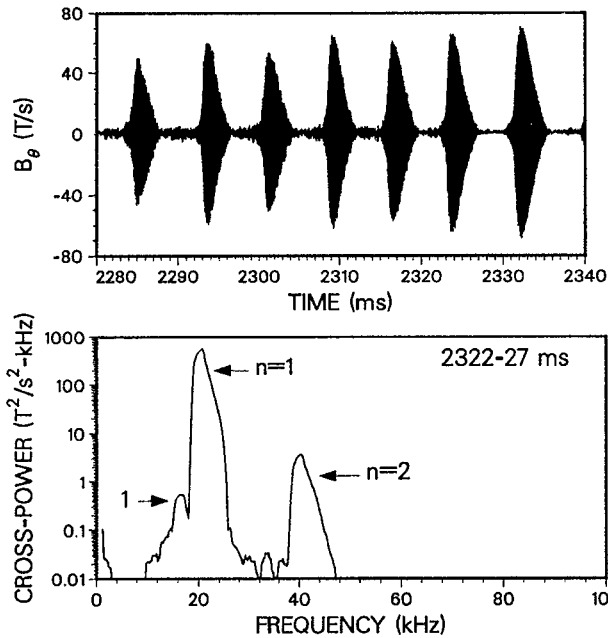


FIG. 1. (top) Signal from an electrostatically shielded Mirnov coil that is mounted near the outboard midplane in a discharge with periodic fishbone bursts. (bottom) Cross-power spectrum between 2322 and 2327 ms for two probes that are separated toroidally by 90° . The toroidal mode number n determined from a toroidal array of eight probes is also given. $B_T=2.1$ T, $I_p=1.6$ MA, $\bar{n}_e=2 \times 10^{13}$ cm $^{-3}$, $P_B=10$ MW, double-null divertor configuration, low-mode confinement.

identification of the time of the bursts) is typically $\leq 10\%$ for regular cycles and 50% for extremely erratic cycles. To quantify the complexity of the Fourier spectrum, we compute FFT's throughout the time record and measure the ratio of the power in the second largest peak in the spectrum P_2 to the power in the fishbone peak P_1 . (Harmonics of the fishbone peak are excluded, of course.) The average value of P_2/P_1 is then computed. Uncertainties of 25% – 60% are typical.

The results of this analysis for the 35 discharges in our database are shown in Fig. 3. A definite correlation between the measured complexity of the burst cycle $(\delta A \delta T)/(\bar{A} \bar{T})$ and the complexity of the Fourier spectrum P_2/P_1 is observed (correlation coefficient $r^2=0.48$). All highly regular cycles $[(\delta A \delta T)/(\bar{A} \bar{T}) < 0.01]$ have pure Fourier spectra ($P_2/P_1 < 0.03$). On the other hand, for a given value of P_2/P_1 , considerable spread in the complexity of the burst cycle is observed.

We have examined our dataset for additional correlations, but none were found. There is no systematic dependence on the toroidal mode number of the perturbing mode, which ranges from $n=0$ – 4 in our data. (Most of the perturbing modes appear to be tearing modes.) Edge localized modes¹⁰ (ELM's) have no discernible effect on the cycle. (This is probably because the fishbone instability is a core instability, while ELM's are an edge instability.) Correlations with B_T and I_p are also absent.

To explain the data, we extend the predator–prey model of Ref. 6 to include periodic perturbations.⁵ Changes in the amplitude of an unstable tearing mode might modify the

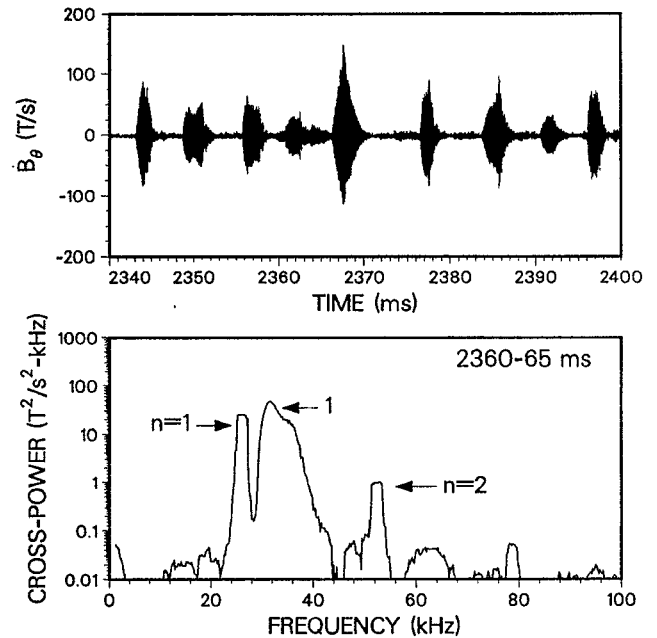


FIG. 2. (top) Signal from a Mirnov coil in a discharge with irregular fishbone bursts. (bottom) Cross-power spectrum between 2360 and 2365 ms, $B_T=2.1$ T, $I_p=1.0$ MA, $\bar{n}_e=4.6 \times 10^{13}$ cm $^{-3}$, $P_B=8$ MW, double-null divertor configuration, very-high-mode confinement.

damping of the beam-driven mode on the background plasma by modifying the current, pressure, or temperature profiles. Or, the tearing mode might enhance the transport of beam ions, either by interacting with the fishbone instability to modify the transport induced by the beam ions, or by introducing its own independent losses. Previous studies of the fishbone instability have shown that both the mode threshold and the induced losses are very sensitive to variations in the q profile,¹¹ so it is plausible that periodic variations in tearing mode amplitude could produce periodic perturbations in parameters that affect the burst cycle. Previous measurements also indicate that tearing mode activity can directly modulate the number of fast ions in the plasma.¹

When expressed in dimensionless variables,⁶ the evolution equations for the mode amplitude a and beam number n are

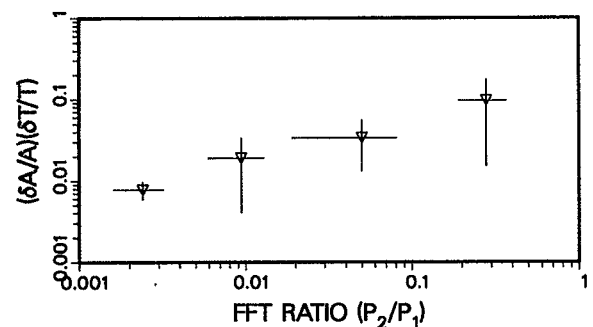


FIG. 3. Irregularity of the burst cycle $(\delta A \delta T)/(\bar{A} \bar{T})$ versus the ratio of the power in the secondary mode to the power in the fishbone mode P_2/P_1 for 35 steady-state discharges with fishbones. The error bars represent the standard deviation of the binned data.

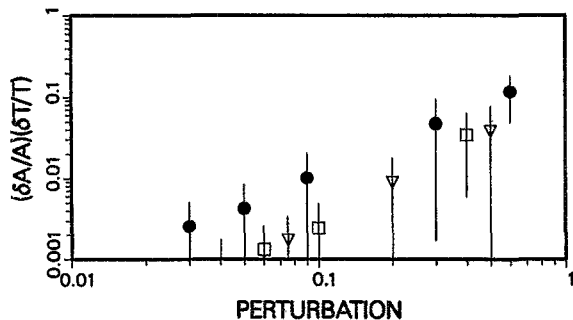


FIG. 4. Irregularity of the burst cycle $(\delta A \delta T)/(\bar{A} \bar{T})$ versus the amplitude of the perturbation for the model equations [Eqs. (1) and (2)]. Each point represents the mean of 12 runs with various mode amplitudes and perturbation frequencies; the error bars represent the standard deviation of the 12 runs. (∇) Perturbations in damping rate δ ; (\square) perturbations in fishbone-induced transport ϵ ; (\bullet) additional losses ζ .

$$\frac{da}{dx} = na + \delta a \sin \omega_{\delta} x, \quad (1)$$

$$\frac{dn}{dx} = 1 - a(1 - \epsilon \sin \omega_{\epsilon} x) + \zeta \sin \omega_{\zeta} x. \quad (2)$$

Here, δ , ϵ and ζ represent perturbations in damping on the background plasma, mode-induced transport, and additional transport, respectively.

We have solved Eqs. (1) and (2) numerically for many values of δ , ϵ , and ζ . Generally, a larger value of perturbation parameter results in a more irregular cycle. The perturbation is most effective at disrupting the cycle when the assumed perturbation frequency (ω_{δ} , ω_{ϵ} , or ω_{ζ}) is comparable to the burst frequency of the unperturbed cycle. To compare with experiment, we create an ensemble of cycles for various values of the perturbation parameters. Each type of perturbation (δ , ϵ , ζ) is considered separately. For each value of δ , ϵ , or ζ , three unperturbed cycles ($a_{\max} = 1.3, 2.1, \text{ and } 3.0$) and four frequencies ($\omega = 0.2, 0.5, 1.0, \text{ and } 2.2$) are used. The resulting value of $(\delta A \delta T)/(\bar{A} \bar{T})$ is calculated for each cycle and the ensemble average is computed.

The results of this analysis are shown in Fig. 4. With the inclusion of perturbations, the model equations [Eqs. (1) and (2)] predict the same sort of behavior observed in the experiment. Large scatter is observed, but the general trend is for larger perturbations to produce more irregular cycles. All three types of perturbations produce the same qualitative behavior although, for a given value of perturbation in the normalized variables, the independent losses tend to have a stronger effect than perturbations in damping rate or mode-induced transport.

The similarity between Figs. 3 and 4 suggests that additional MHD modes disrupt the fishbone cycle through perturbations in the growth rate or loss rate. Our analysis does not indicate how the MHD modes perturb the rate; indeed, the theoretical results indicate that *any* type of periodic perturbation can account for the data. This may explain why no systematic dependence on the toroidal mode number of the

perturbation is observed. The theoretical analysis also indicates that the frequency of the perturbation can affect the cycle. In Fig. 3, only the amplitude of the perturbation (P_2/P_1) is considered. Variations in the frequency of the perturbing mode may account for some of the scatter in Fig. 3.

It is unlikely that the secondary MHD instability is another beam-driven mode. Theoretically, in a model system with two modes that prey upon the fast-ion population, the mode with the higher threshold for instability quickly decays. The analogous result is well known in biology,¹² and accounts for the observation that most ecosystems have a dominant predator. Experimentally, however, two beam-driven modes do sometimes coexist. For example, concurrent periodic bursts of TAE activity and fishbone activity are not uncommon in DIII-D discharges with $B_T < 1.4$ T (cf., Fig. 6 of Ref. 6). Usually, one instability is dominant and seems to trigger the weaker mode, perhaps by modifying the gradient of the fast-ion pressure. This phenomenon is not consistent with zero-dimensional predator-prey models. Spatially dependent models are beyond the scope of our study.

In conclusion, the complexity of the burst cycle correlates with the presence of perturbing instabilities in DIII-D. Since an extended predator-prey model predicts irregular burst cycles in the presence of perturbations, the data are consistent with the notion that particle loss is the dominant saturation mechanism for beam-driven instabilities.

ACKNOWLEDGMENTS

The support of the DIII-D team and helpful discussions with A. Turnbull and R. White are gratefully acknowledged.

This work was supported by Subcontract No. SC-L134501 of U. S. Department of Energy Contract No. DE-AC03-89ER51114.

¹W. W. Heidbrink and G. J. Sadler, Nucl. Fusion **34**, 535 (1994) and references therein.

²L. Chen, R. B. White, and M. N. Rosenbluth, Phys. Rev. Lett. **52**, 1122 (1984).

³B. Coppi, S. Migliuolo, and F. Porcelli, Phys. Fluids **31**, 1630 (1988).

⁴R. B. White, *Theory of Tokamak Plasmas* (North-Holland, Amsterdam, 1989), p. 280.

⁵D. Borba, M. F. F. Nave, and F. Porcelli, in *Theory of Fusion Plasmas* (Commission of the European Communities, Brussels, 1992), p. 285.

⁶W. W. Heidbrink, H. H. Duong, J. Manson, E. Wilfrid, C. Oberman, and E. J. Strait, Phys. Fluids B **5**, 2176 (1993).

⁷J. L. Luxon and L. G. Davis, Fusion Technol. **8**, 441 (1985).

⁸W. W. Heidbrink and G. Sager, Nucl. Fusion **30**, 1015 (1990).

⁹During a 60 ms time window, variations in I_p , \bar{n}_e , stored energy W_{dia} , and the mean value of the neutron emission of $\approx 5\%$ and variations in a central visible bremsstrahlung signal of $< 10\%$.

¹⁰F. Wagner, M. Keilhacker, the ASDEX Team, and the NI Team, J. Nucl. Mater. **121**, 103 (1984).

¹¹D. W. Roberts, R. Kaita, F. Levinton, N. Asakura, R. Bell, M. Chance, P. Duperrex, G. Gammel, R. Hatcher, A. Holland, S. Kaye, C. Kessel, H. Kugel, B. LeBlanc, J. Manickam, M. Okabayashi, S. Paul, N. Pomphrey, E. Powell, N. Sauthoff, S. Sesnic, H. Takahashi, and R. White, Phys. Rev. Lett. **71**, 1011 (1993).

¹²A. Rescigno and I. W. Richardson, in *Foundations of Mathematical Biology*, edited by R. Rosen (Academic, New York, 1973), Vol. III, Chap. 4.